Heritage Science

RESEARCH Open Access

Water-holding properties and electrochemical characterization of the soil under the Grand Deliverance Hall of the Chongshan Temple, Taiyuan City, China: providing the basis for preventing groundwater erosion in historic buildings

Yi Lu[1], Xiangling Bai[2*], Xiaolong Wang[1], Lin Han[1], Xiaojian Bai[3], Pengju Han[2*] and Yijing An[2]

Abstract

Many historic buildings are at serious risk of deterioration due to changes in the moisture content of the soil under the buildings. Based on the typical deterioration problems of the Grand Deliverance Hall and the cultural relics in the hall, this study analyzes and concludes that the main factor affecting the generation and development of deterioration is groundwater erosion through environmental monitoring and geotechnical engineering investigation. The impact of changes in moisture content on the water-holding properties and pore distribution of the soil under the cultural-relics buildings was further assessed. Then, combined with the soil property, our study provides a novel and effective way to monitor and reflect the water-holding properties of the soil using electrochemical detection. The connected pore resistance and matrix suction decrease with the increase in the moisture content, both showing a power function law. Changes in moisture content cause changes in the thickness of the double electric layer, which in turn affects the connected pore resistance and matrix suction of soil. The greater the connected pore resistance, the greater the matrix suction and the water holding capacity. Finally, based on the research of this study and the conservation ideology of cultural relics that respects the original and minimizes intervention, protection recommendations to prevent groundwater erosion are proposed in order to provide guidance for future research.

Keywords Historic buildings, Water-holding properties, Electrochemical characterization, Preventive conservation

*Correspondence:
Xiangling Bai
jelly18235339657@163.com
Pengju Han
13834569544@163.com
Full list of author information is available at the end of the article

Graphical Abstract

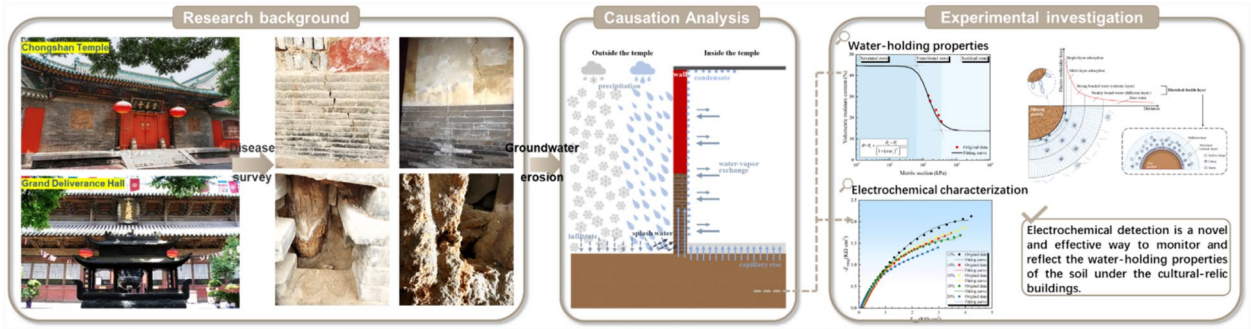

Introduction

In recent years much attention has been given to the preventive conservation of the cultural-relic buildings. Many international organizations and scholars, such as the World Heritage Committee, International Center for the Study of the Preservation and Restoration of Cultural Property, and International Council on Monuments and Sites, are committed to adhering the concepts of prioritizing conservation and further exploring how to conduct inheritance and preservation of historic buildings using scientific methods [1–5].

Historic buildings are mostly composed of brick-stone-wood-soil materials. Due to the long history of the buildings and the influence of the change in the environment, some deterioration problems arise, such as water erosion, peeling off, crack and lower stability [6–9]. Changes in the environmental are one of the most important factors that directly influence the deterioration problems. Excessive humidity in historic buildings can cause material corrosion and other deterioration problems [10, 11], while low humidity can cause cracking and deformation [12]. Temperature changes in the environment lead to shrinkage, deformation, cracking, and chemical deterioration of the cultural relics [13–16]. These deterioration problems can have a significant impact on the durability and heritage value of the historic buildings. Therefore, to protect historic buildings, it is crucial to identify the causes of deterioration. The Venice Charter (International Charter for the Conservation and Restoration of Monuments and Sites) and related protection principles [17, 18] stipulate that any research work should not damage the original structure of the cultural heritage, which makes it difficult to study the causes of deterioration and preventive protection.

The science and technology provide important support for the protection and study of historic buildings. In recent years, scholars have widely used indoor tests, field monitoring, and numerical simulation and analysis to explore and study the causes of historic buildings deterioration [19–21], which have significant research value for the understanding of the deterioration mechanisms and the provision of protective measures. Aiming at the influence of environmental changes, scholars have adopted non-destructive detection methods to study the structural damage characteristics of historic buildings from different theoretical levels [22, 23], and to establish safety-assessment methods.

For historic buildings, it is essential to scientifically assess the state of the environment in which the buildings are located, determine the deterioration causes, and use scientific monitoring techniques [24–27]. Research and practical experience in regulating the upper building environment in order to achieve optimal preservation has been relatively mature, but there is fewer research on the water-holding properties of the soil under the historic buildings. Applying science and technology to reflect the changes in the water environment of the soil under buildings, so that the non-destructive tests from qualitative determination gradually changed to quantitative characterization, and quickly determine the conditions of the soil are prerequisite and necessary link to enrich the safety assessment methods of historic buildings.

Therefore, in order to better understand the direct influence of change in the water environment of the soil under historic buildings, and based on the need for the protection and development of the historic buildings, this study investigates the water-holding properties and electrochemical characteristics of the soil under the Grand Deliverance Hall of the Chongshan Temple, Taiyuan city, China. The study summarizes the main deterioration problems of the Grand Deliverance Hall and the cultural relics in the hall, analyzes and concludes that the main factor affecting the generation and development of deterioration is groundwater erosion through environmental

monitoring and geotechnical engineering investigation. The impact of changes in moisture content on the water-holding properties and pore distribution of the soil under the cultural-relics buildings was further assessed. Then, this study provides a novel and effective way to monitor and reflect the water-holding properties of the soil using electrochemical detection. Finally, based on the research of this study and the conservation ideology of cultural relics that respects the original and minimizes intervention, protection recommendations to prevent groundwater erosion are proposed in order to provide guidance for future research.

Case study

Overview of the Chongshan Temple, Taiyuan City, China

The Chongshan Temple (Fig. 1) is located in Taiyuan City, Shanxi Province, and represents the Baima Temple of the Tang Dynasty and the Chongshan Buddhist Temple of the Ming Dynasty in China. The temple is 550 m long from north to south by 250 m wide from east to west, with a total area of 140,000 m^2, and its layout includesthe bell tower, the wing room, and the Grand Deliverance Hall. The Grand Deliverance Hall is official-style wooden building of the early Ming Dynasty in China, which is highly reflecting the development of ancient culture and the rise and fall of religions. It was identified as a national key cultural relics protection unit in 2013. The Chongshan Temple also preserves many historical relics for the study of ancient Chinese culture, including the Buddhist sutras reflecting the history of Chinese woodblock printing, the copy of a mural mapping the history of Chinese painting, and three clay statues of bodhisattvas embodying the art of Chinese sculptures.

Preliminary analysis of the deterioration problems

Deterioration problems

Precious relics such as ancient wooden buildings and statues, are sensitive to the preservation environment due to the particularities of the materials and structures [28, 29]. Different types and degrees of deterioration problems have occurred in the Grand Deliverance Hall, significantly affecting the value and stability. The main deterioration problems are as follows:

- The walls and floors of the hall have suffered from salt efflorescence and crack damage (Fig. 2), while the walls are tilted with a high front and a low back, or with a low center and two high ends.
- Uneven settlement and decay have occurred in the interior of the hall and the columns in the wall, and the decay of the columns in the wall is particularly severe (Fig. 2).
- Statues in the hall have suffered from the loss of pigment layer and fracture damage (Fig. 2). And the deterioration problem of the bottom part of the statues, which is near the floor, is more serious.

Preliminary analysis of causes

Environment monitoring Environmental factors influencing the stability of cultural relics mainly included: moisture uptake, temperature variation and wind erosion. Among them, the change of temperature and humidity is one of the most important factors affecting the preservation of cultural relics [30, 31]. Therefore, the seven temperature and humidity data loggers were set in the Grand Deliverance Hall to record the hall temperature and humidity in real-time. Monitoring in accordance with the

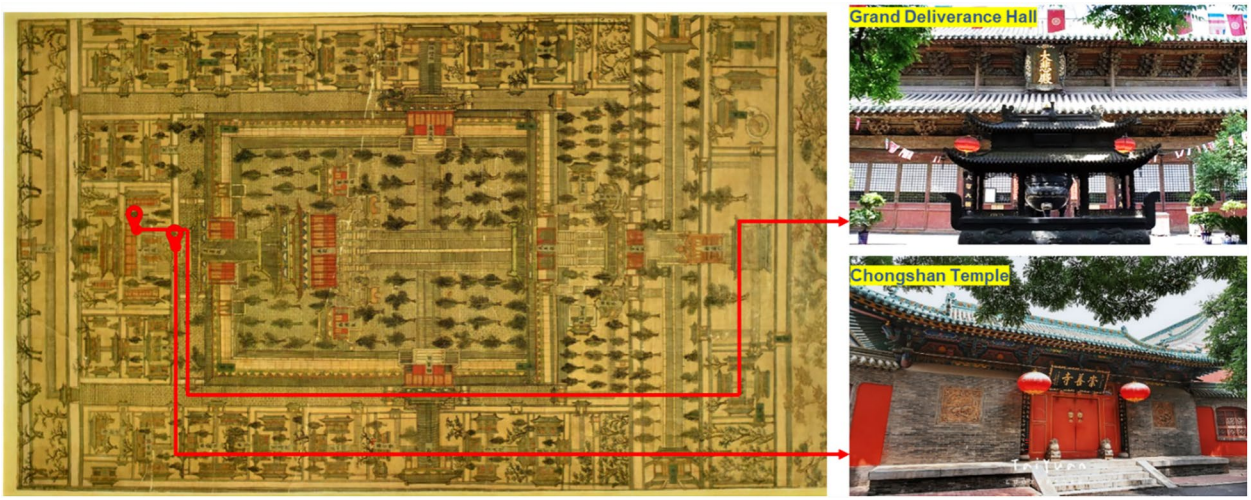

Fig. 1 Sanjin (Shanxi) ancient temple: the Chongshan Temple

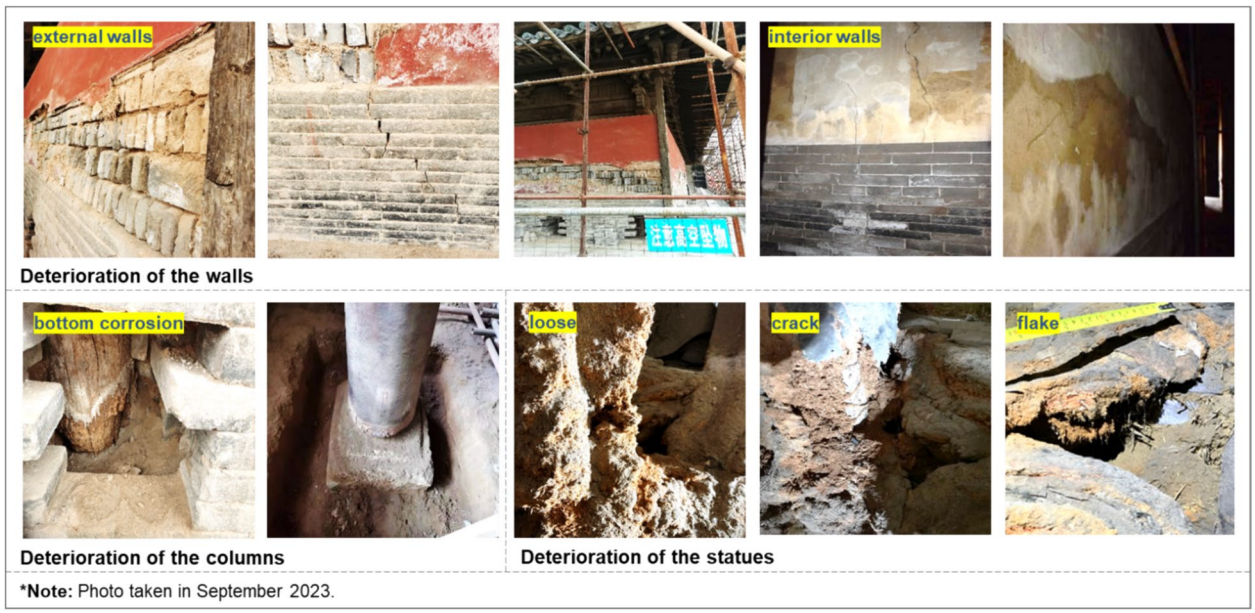

Fig. 2 Deterioration problems of cultural relics in the Great Deliverance Hall

Law of the Cultural Relics Protection Law of the People's Republic of China and the Protection Guidelines of the Cultural Relics in China. The data collection period was set from 1 January 2023 to 31 December 2023. The seven sets of data are basically consistent. The temperature and humidity monitoring data for the Grand Deliverance Hall are shown in Fig. 3.

As shown in Fig. 3, the trends in temperature and humidity changes in the hall are more consistent. The temperature inside the hall was at its lowest in December, and then slowly increased to reach a maximum temperature of 27.15 °C in July. The relative humidity in the hall reaches 50% or more most of the year, with lower humidity of about 40% in April through May relative to the other months.

Geotechnical investigation Exploring the characteristics of the soil under the historic buildings is a prerequisite for further clarifying the causes of the deterioration problem. Geotechnical investigation of the soil under the Grand Deliverance Hall in accordance with the relevant provisions of the Code for Investigation of Geotechnical Engineering and Code for Investigation of Earthen Heritage Sites Conservation Works. The investigation concluded that the soil texture is mainly silty soil with high moisture content. The soil contained more chloride and sulfate ions. With the increase in investigation depth, the moisture content and the pore ratio of the soil increases, the density decreases.

Causes analysis The Chongshan Temple of Taiyuan City is located in the temperate continental monsoon climate area, which has the characteristics of four distinct seasons and the same period of rain and heat. In the spring (March to May), as the temperature rises, the water in the soil gradually evaporates, resulting in a lower humidity and lower moisture content. Precipitation is highest during the summer (June to August), and the humidity in the hall and soil are at the highest. In the autumn (September to November), as the temperature drops, precipitation and the humidity in the hall decreases. In the winter (December to February), as precipitation continues to decrease, temperature and humidity first continue to fall and then rise. It can be preliminarily concluded that the temperature and humidity changes in the hall have significant correlated with the temperature and humidity changes in the soil under the hall. The caused for the deterioration of the hall and the cultural relics may include the following aspects.

(1) The main building materials for the Grand Deliverance Hall and the cultural relics are brick, block and wood, which showed highly water absorption. Under the action of groundwater erosion, capillary pores pressure is formed inside the material pores. At the same time, capillarity effect causes internal expansion stress on the material pores, and the building materials have flaking and cracks due to

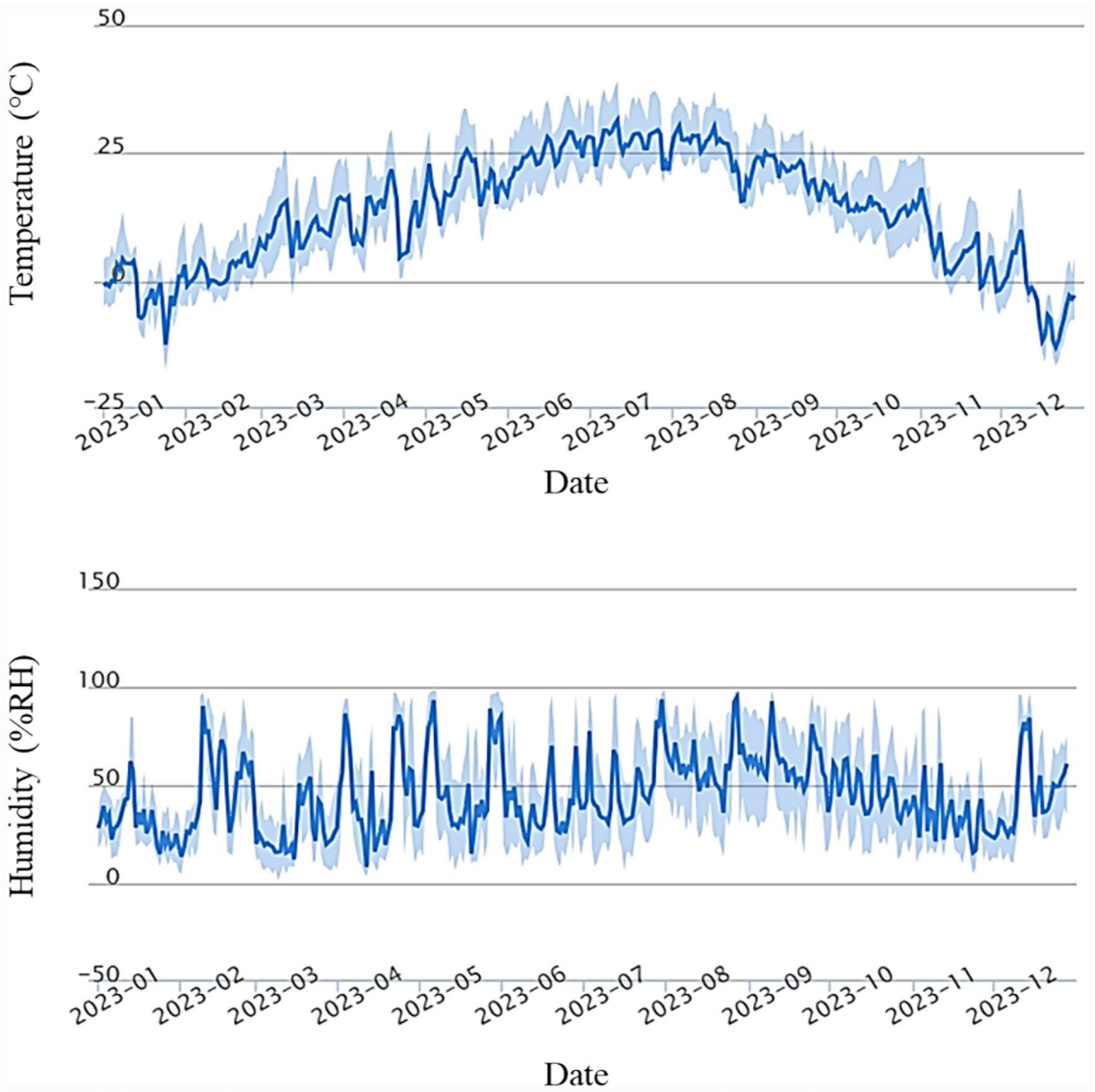

Fig. 3 Temperature and humidity data of the Grand Deliverance Hall

internal stress changes [32]. The schematic diagram of groundwater erosion is shown in Fig. 4.

(2) Soluble salts in the soil under the influence of moisture migration. Can cause material cracking, severe corrosion occurred along the bottom of the column and other problems, thus reducing the mechanical properties of the material and affecting the overall stability of the structure.

(3) External temperature changes could aggravate the stress formed by the internal moisture of the material on the pore walls, which in turn damages the microstructure. The wind erosion could lead to the coursing of the material surface texture and increase the surface roughness by forming the wind erosion dent, which also affects the further groundwater erosion.

Through the above comprehensive analysis, we can conclude that the main factor affecting the generation and development of deterioration problems of the Grand Deliverance Hall and the cultural relics in the hall is groundwater erosion. Moreover, climatic factors such as temperature changes and wind erosion can exacerbate the severity of deterioration. Therefore, in order to comply with the specificity of cultural relics conservation, it is necessary to use a non-destructive monitoring method to reflect the water-holding properties and changes in the moisture content of the soil under the hall.

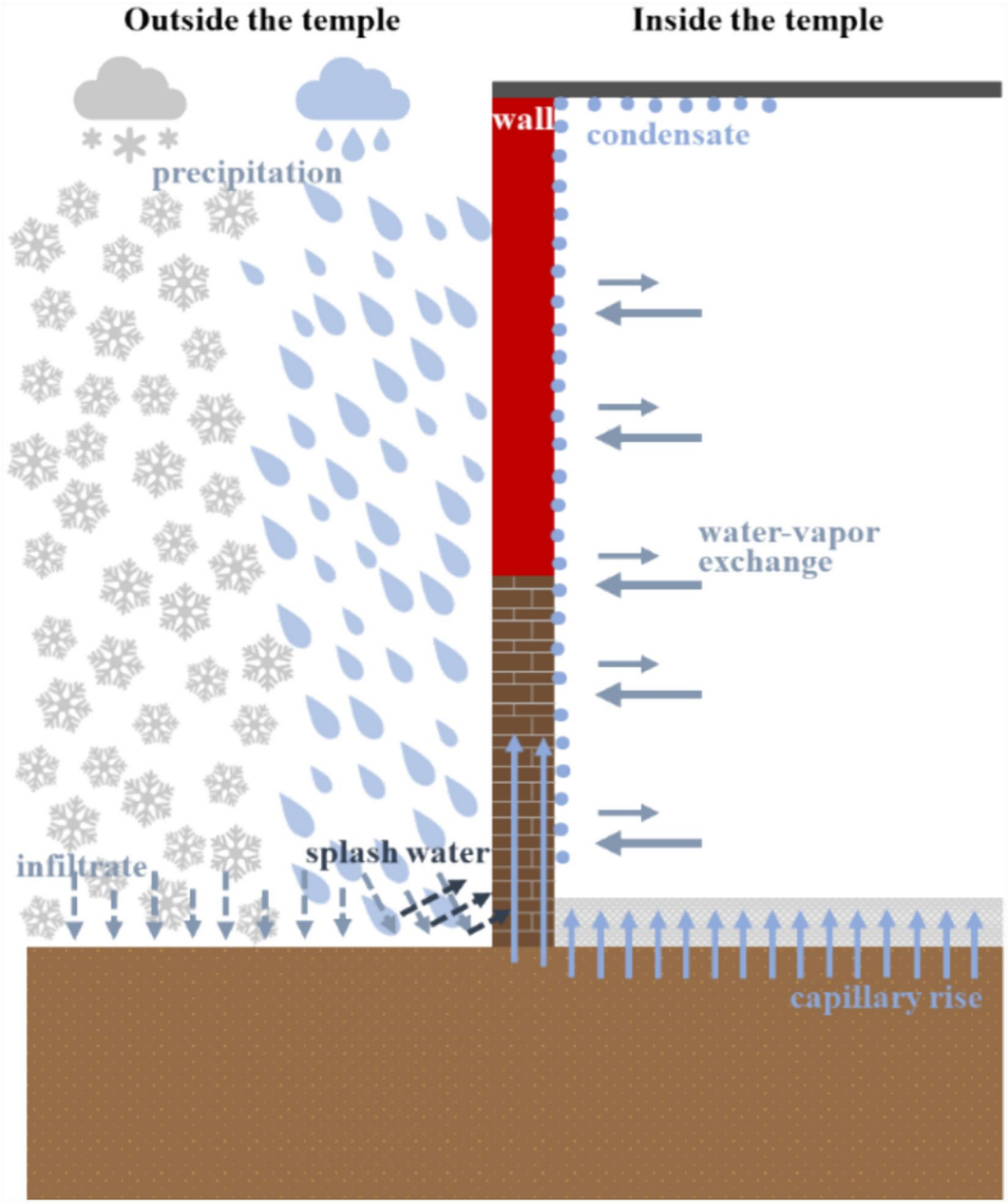

Fig. 4 Schematic diagram of groundwater erosion in the Grand Deliverance Hall

Research aims

At present, the protection of cultural relics is developing from salvage protection to preventive protection. The main factor affecting the deterioration problem of the Grand Deliverance Hall is groundwater erosion, therefore, the use of non-destructive methods to reflect the water-holding properties and moisture changes of the soil under the hall is a necessary preparation for the proposal of targeted repair measures as well as the formation of a comprehensive conservation ideas.

The research objectives of this paper are:

(1) Clarifying the water-holding properties and pore water distribution of the soils under the hall.
(2) Utilizing non-destructive detection methods to reflect changes in the moisture content and water-holding properties of the soils under the hall.

(3) Providing the scientific basis for monitoring and conservation of the cultural-relic buildings are at serious risk due to changes in the water environment of the soils under the historic buildings.

Materials and methods

Test materials

According to the geotechnical investigation, the soil texture of the investigation range is mainly silty soil. In view of the protection of cultural relics, a large number of soil samples under the Grand Deliverance Hall cannot be removed for testing, so after comparing the soil texture in the surrounding range, choose the 2 # soil samples as the test materials. The schematic diagram of sampling locations based on the actual location of the Grand Deliverance Hall is shown in Fig. 5, and the basic properties of the soils are shown in Table 1.

The X-ray Diffraction analysis of the soil samples under the Grand Deliverance Hall and the soils soil samples from the sampling site 2 showed that the minerals in soils were mainly comprises of quartz, anorthosite, calcite and clay minerals (chlorite and illite), and the mineral contents of these two soil samples were relatively consistent. Figure 6 shows the XRD pattern of the soil samples used for testing, the content of minerals is presented in a tabular form. Among them, quartz and calcite are weakly hydrophilic minerals, which have little effect on the adsorbed water in the soil. Chlorite and illite are both hydrophilic clay minerals, which have a large effect on the adsorbed water in the soil, and are the main source of soil suction [33].

Test methods

Sample preparation

The soil samples were naturally air-dried, crushed, and sieved through a 2 mm soil sieve before being placed in a blast drying oven to dry the soil at 105 ℃ for 12 h. To clarify the effect of varying moisture contents on soil properties, and in conjunction with the actual situation, the initial dry density of the soil samples was determined to be 1.55 g/cm^3 and five different initial gravimetric moisture contents were selected as test variables (12, 14, 16, 18, and 20%). The dried soil samples were re-mixed with the target moisture and kept in an airtight container at constant temperature and humidity for 24 h to ensure uniform distribution of water in the soil pore.

Water-holding property tests

The water-holding properties of soils are commonly described by curves of the volumetric moisture content versus matrix suction. Therefore, in this study, the total suction and conductivity of soils were tested using a Dewpoint Potential Meter (WP4C, Pullman, WA, USA) and a Conductivity Meter (DDS-307A, Shanghai,

Fig. 5 Schematic diagram of sampling locations

Table 1 The basic properties of soils

Sample site	ω (%)	ρ_d (g/cm^3)	e –	S_r (%)	$a_{1\text{-}2}$ (MPa^{-1})	$E_{s1\text{-}2}$ (MPa)	W_L (%)	W_P (%)	I_P –
Within the survey area	17.6	1.55	0.74	82.7	0.30	6.12	25.0	16.4	8.6
1#	16.4	1.47	0.68	69.8	0.23	3.60	24.0	16.1	7.9
2#	17.3	1.51	0.75	79.4	0.29	6.27	24.8	16.2	8.6
3#	19.9	1.61	0.82	93.0	0.47	7.70	26.4	16.9	9.5
4#	15.8	1.45	0.61	64.2	0.20	3.43	23.7	15.9	7.8
5#	20.7	1.62	0.69	97.6	0.27	6.40	33.7	19.3	14.4
Sampling schematic									
Within the survey area	1#		2#		3#		4#		5#

ω represents the natural moisture content, ρ_d represents the dry density, e represents the pore ratio, S_r represents the saturation, $a_{1\text{-}2}$ represents the coefficient of compression, $E_{s1\text{-}2}$ represents the modulus of compression, W_L represents the liquid limit, W_P represents the plastic limit, I_P represents the plasticity index

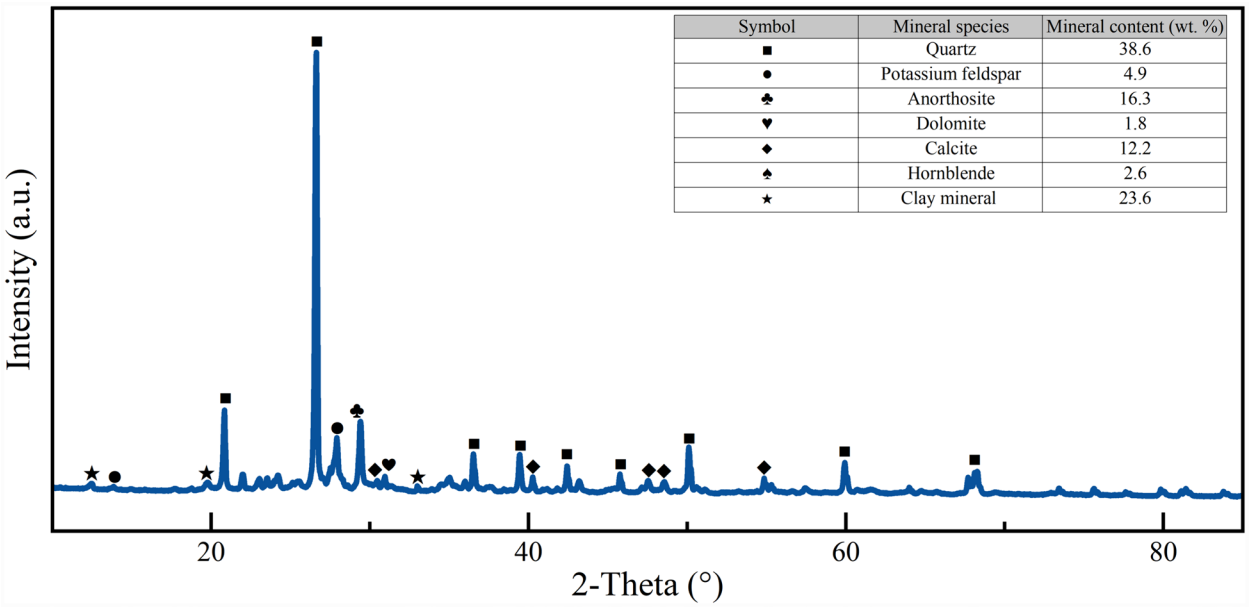

Symbol	Mineral species	Mineral content (wt. %)
■	Quartz	38.6
●	Potassium feldspar	4.9
♣	Anorthosite	16.3
♥	Dolomite	1.8
◆	Calcite	12.2
♠	Hornblende	2.6
★	Clay mineral	23.6

Fig. 6 The XRD pattern of the soil used for testing

China). The WP4C meters was turned on for 30 min before the test, calibrated to ensure the test accuracy, and selected the test mode as Continuous Mode. The soil samples for suction test were cylinders with a diameter of 38 mm and a height of 10 mm.

Electrochemical test

The CorrTest CS350 Electrochemical Workstation (CorrTest Instruments, Wuhan, China) was used for electrochemical impedance spectroscopy (EIS) test of the soil. The electrochemical behavior of soil was investigated by using a three-electrode system, a copper plate electrode as the working electrode, platinum filament as the counter electrode, and a saturated calomel electrode (SCE) as the reference electrode. The working electrode was in advance sealed with epoxy to ensure the tested area of 1.0 cm^2 and ground with SiC abrasive paper, and then ultrasonically cleaned with ethyl alcohol, dried in the air. To minimize the iR-drop at the soil-electrode interface, the distance between the electrodes was set close to each other. Before the test, the instrument needed to be turned on for at least 20 min to minimize the temperature drift, and the test was started with the open-circuit potential stabilized to ensure accuracy and reliability of test data.

The amplitude for EIS test was 10 mV sine wave voltage, and the scanning frequency range was 10^5–10^{-1} Hz. Experimental data of the EIS were analyzed by Zview2 software. The reliability of the impedance spectra was verified by checking the linearity condition and determining the causality condition by Kramers–Kronig transforms.

Sample preparation and testing methods refer to the Standard Geotechnical Test Method and the Technical Specification for Conservation Tests on Earthen Sites. The electrochemical testing was performed according to literature concerned [34–37]. All tests were repeated 3 times to increase the scientific consistency of the results.

Results and discussion

Water-holding properties test

Calculation principles

Calculation of total suction The saturated vapor pressure at the dew point temperature of the soil was measurable by the Dewpoint Potential Meter. And the total suction (Ψ) of the soil can be calculated from the Kelvin equation (Eq. 1), where the total suction, is the sum of the matrix suction and osmotic suction.

$$\Psi = \frac{RT}{M_W} In \frac{e_s(T_d)}{e_s(T_s)} \tag{1}$$

where, $e_s(T_d)$ is the saturated vapor pressure at the dew point temperature, kPa; $e_s(T_s)$ is the saturated vapor pressure at the sample temperature, kPa; R is the universal gas constant, 8.314 J/(mol·K); T is the absolute temperature, ℃; M_W is the molar mass of water, g/mol.

Table 2 Moisture contents of soil samples (%)

ω	Measured gravimetric moisture contents	Volumetric moisture content
12	11.81	18.31
14	13.69	21.22
16	15.57	24.13
18	17.84	27.65
20	19.72	30.57

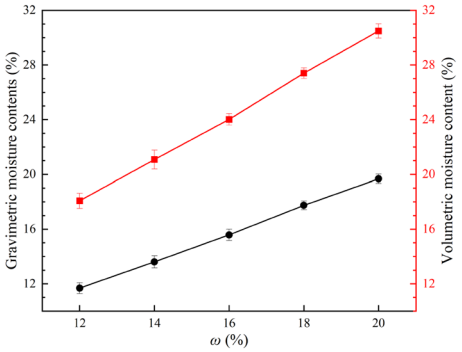

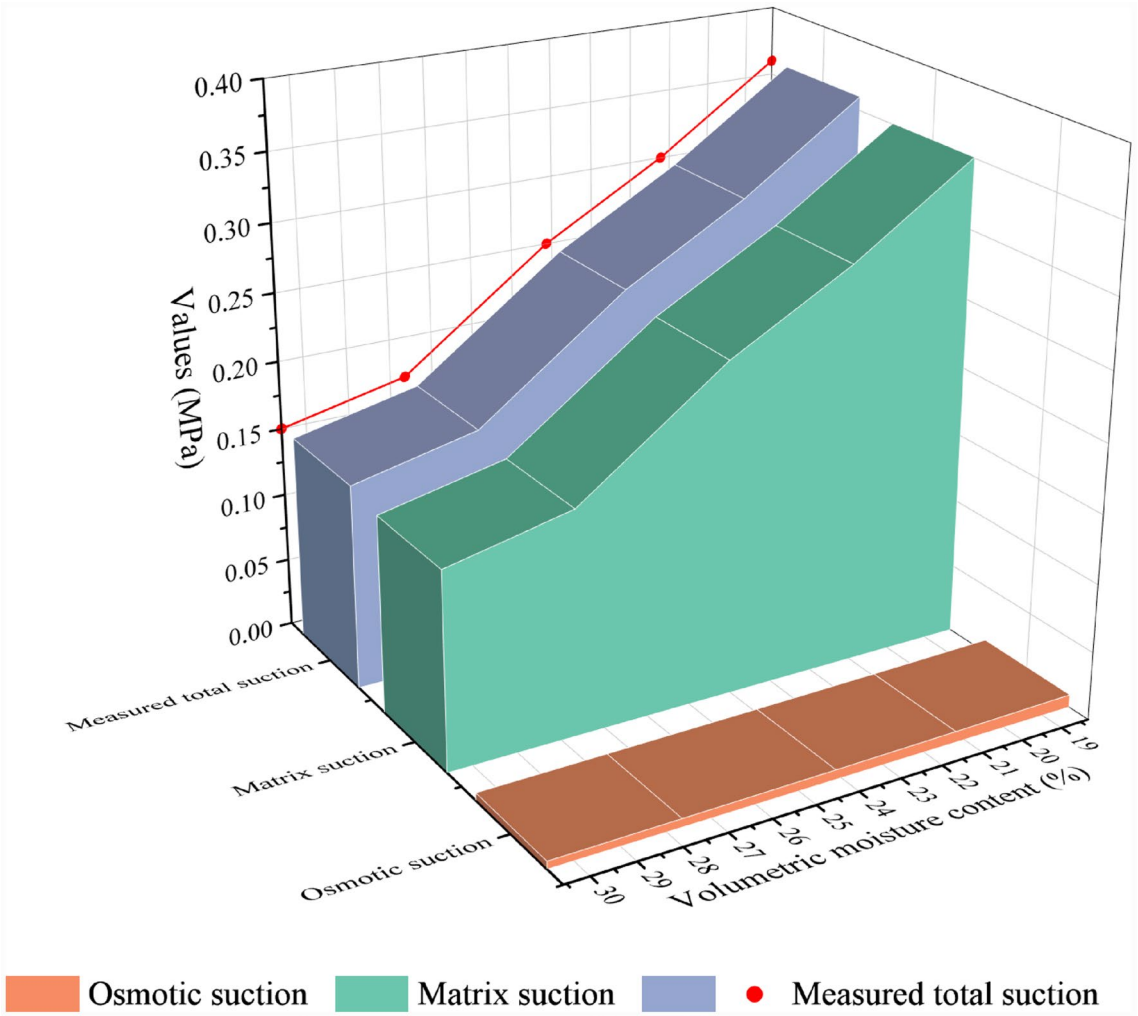

Fig. 7 Total suction, osmotic suction and matric suction of soil samples

Calculation of osmotic suction The osmotic suction of soil saturated extracts (Ψ_{os}) was calculated using Eq. 2 after measuring the electrical conductivity of the soil saturation extract (E_c), and the actual osmotic suction of the soil (Ψ_θ) was then calculated using Eq. 3. The volumetric moisture content (θ) in Eq. 3 can be calculated by using Eq. 4.

$$\Psi_{os} = -0.036E_c \tag{2}$$

$$\Psi_\theta = \Psi_{os}\frac{\theta_s}{\theta} \tag{3}$$

$$\theta = \frac{\omega\rho_d}{\rho_\omega} = \frac{V_W}{V} \tag{4}$$

where, θ_s is the saturated volumetric moisture content of the soil%; ω is the gravimetric moisture contents of the soil, %; ρ_ω is the density of distilled water, 1.0 g cm^3.

Effect of changes in moisture content on matrix suction Due to the small size of the soil samples, the moisture content of the soil will change during the testing process. Therefore, at the end of the measurement of the total suction, the soil samples were dried again and the actual gravimetric moisture contents was calculated to obtain. The result of mean electrical conductivity ($\overline{E_c}$) of the saturated extract is 158.4 μS/cm, so the Ψ_{os} is 5.70×10^{-5} MPa. The volumetric moisture contents of the soil samples calculated according to Eq. 1 to Eq. 3 are shown in Table 2, and the total suction is shown in Fig. 7.

The two indexes of the volumetric moisture content (θ) and saturation (S_r) are usually used to reflect the state of water in the soil and the filling situation. Where the θ is the ratio of the volume of pore water (V_w) to the total volume of the soil (V), and the S_r is the ratio of the volume of water to the volume of pore in the soil.

According to Eq. 4 to Eq. 6, it can be seen that the increase of ω means the increase of θ and S_r.

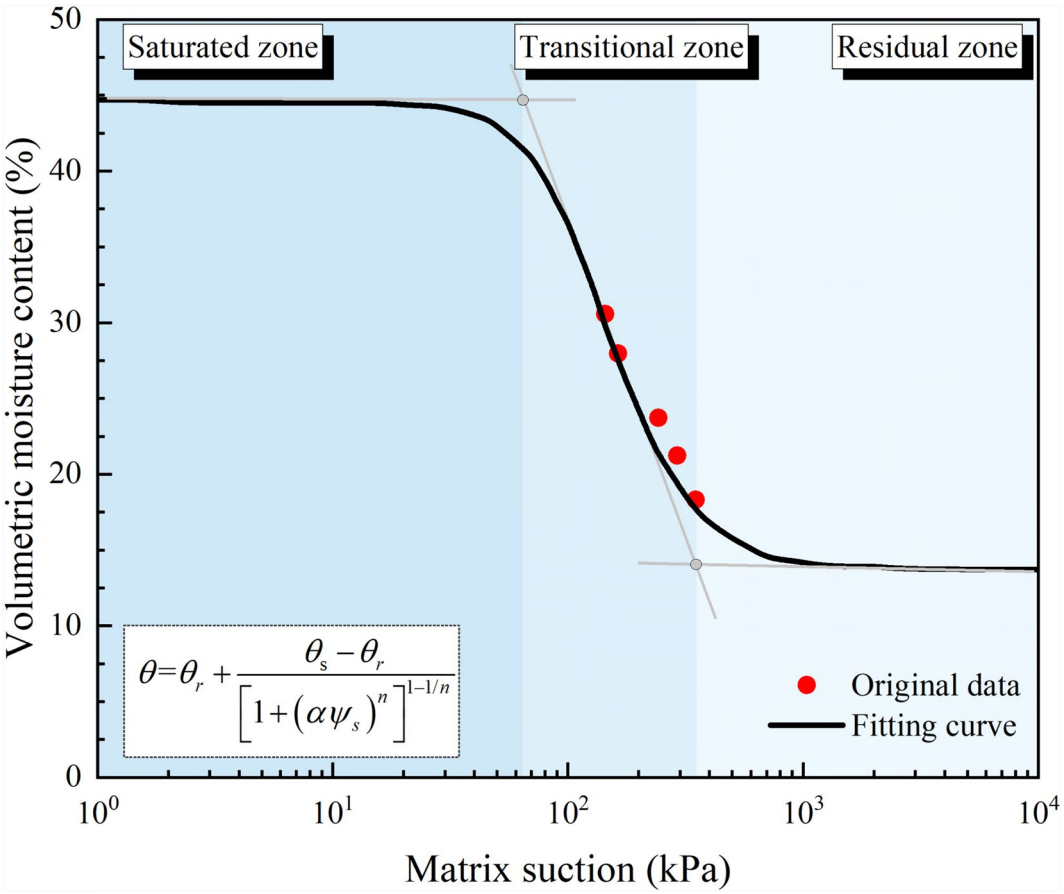

Fig. 8 SWCC after van-Genuchten model fitting

$$S_r = \frac{d_s \omega}{e} \tag{5}$$

$$\rho_d = \frac{d_s \rho_\omega}{1+e} \tag{6}$$

where, d_s represents the relative density of the soil, 2.7; e represents the void ratio of the soil.

According to the principle that the that matrix suction is equal to the difference between total and osmotic suction, the relationships between the suction and volumetric water content of soil samples with different initial water contents were calculated and shown in Fig. 7, where the volumetric water content is calculated from Eq. 4 to Eq. 6. It can be seen that the volumetric water content has a significant effect on the total suction and matrix suction of the soil. When the volumetric water content was lower, the total suction and matrix suction were greater.

Soil–water characteristic curves (SWCC)

Using the classical van-Genuchten model, the SWCC of soil samples with different moisture contents were obtained (Fig. 8) to visualize the variation of matrix suction with the volumetric moisture content. Where, θ, θ_r, and θ_s are the volumetric moisture content, residual moisture content, and minimum suction moisture content, respectively. The correlation coefficient R^2 of the van-Genuchten model was 0.987.

The SWCC can be categorized into saturated, transitional, and residual zones, which reflect the water-holding properties of the soil [38]. When the volumetric moisture content is low and approaches the residual volumetric moisture content, the soil is close to being completely dry and smaller changes in the moisture content cause more sensitive changes in matrix suction. This is because there are many large pores in the soil with good pore connectivity, the particles do not easily come into contact each other. Clay minerals such as quartz, feldspar and illite in the soil particle component, have strong surface energy. The electric field generated by its charge adsorbed on the surface acts in conjunction with the van der Waals force to make the adsorption of the adsorbed water on the soil surface extremely strong and has a large effect on the matrix suction with the change of the moisture content, forming an adsorbed water layer with good water-holding property [39].

As the volumetric moisture content increases, the SWCC in the transitional zone becomes steeper and the change in matrix suction is smaller. This is due to the emergence of a bound water layer, which together with the adsorbed water layer constitutes membrane water. The bound water is subjected to an attractive force that decreases with increasing distance from the soil surface, so it can be divided into the strong bound water layer and the weak bound water layer [40, 41]. When the moisture content continues to increase to the extent that the free water appearing in the soil, the SWCC reaches the saturated zone and became flatter. Matrix suction continues to decrease until the soil is completely saturated, at which time the volumetric moisture content is the saturated volumetric moisture content.

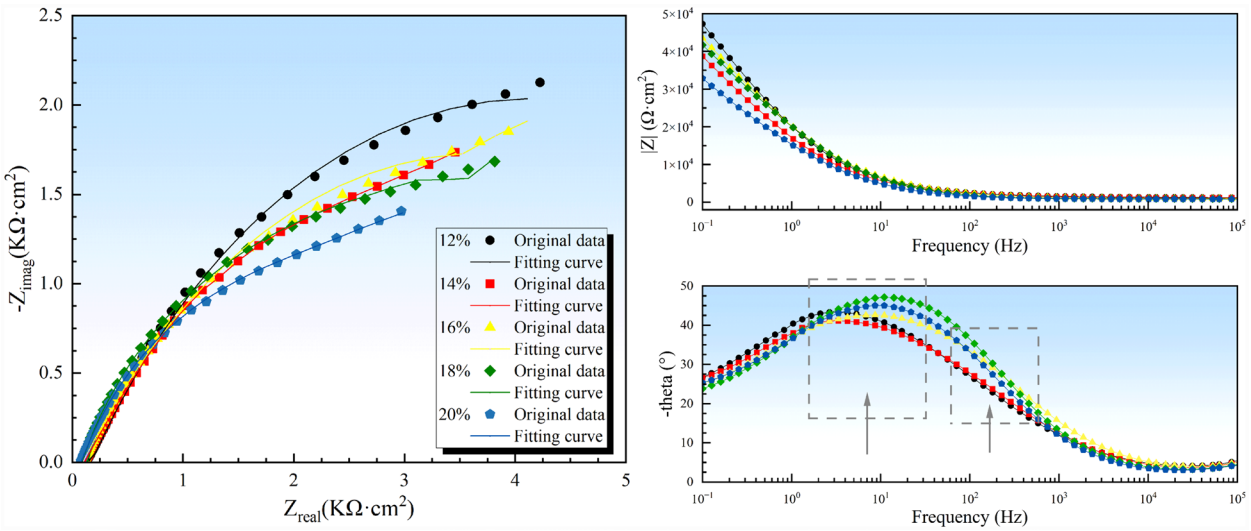

Fig. 9 Electrochemical impedance spectra of soil samples with different moisture contents

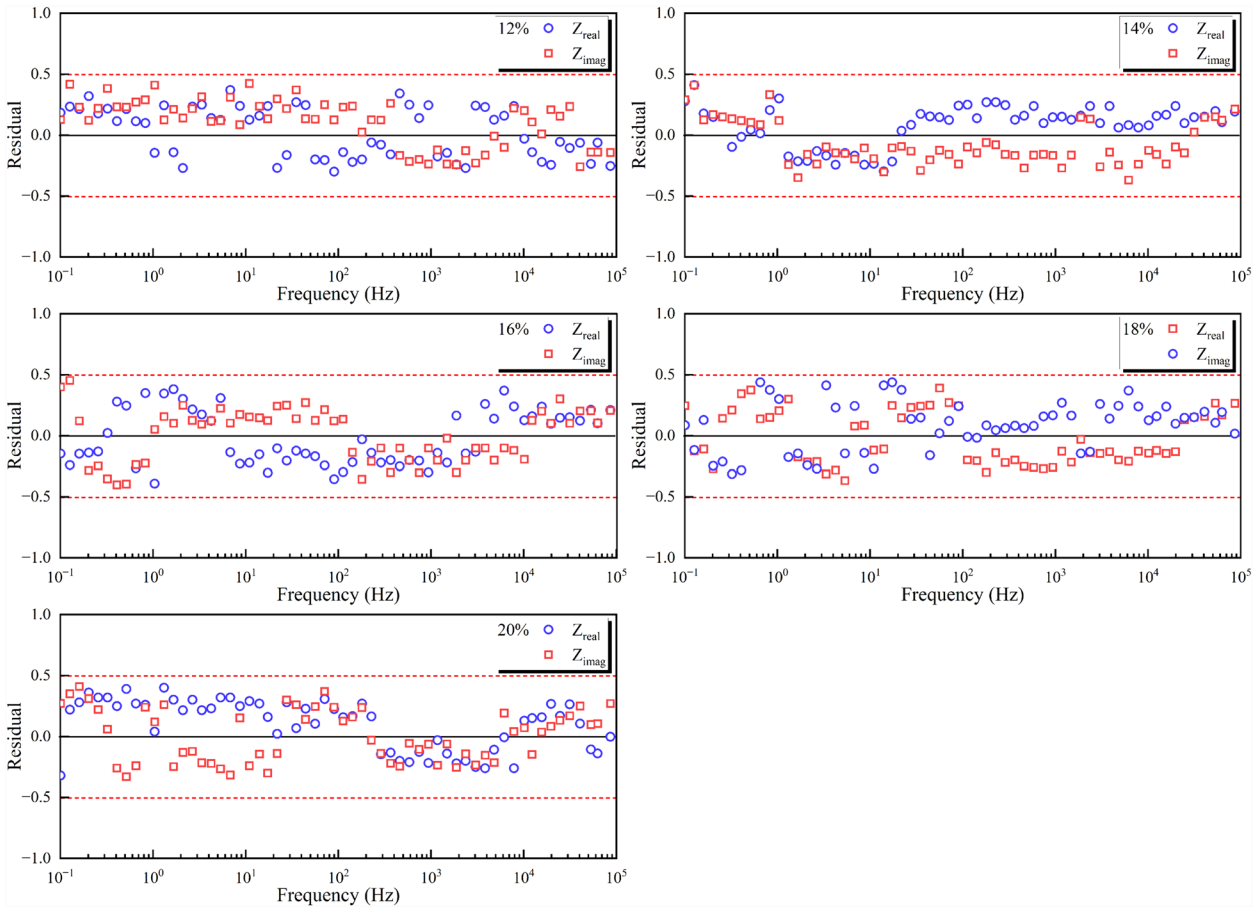

Fig. 10 Residuals plot of the electrochemical data of the soil samples

Electrochemical test

Test principle

Electrochemical Impedance Spectroscopy (EIS) can characterize the electrochemical systems by applying a variable frequency sine electric potential perturbation to the study the current response [42, 43]. The microscopic pore structure within the soil is closely related to its water-holding properties. According to the EIS data

Table 3 Parameter values for equivalent circuit model fitting

ω	R_{ct}	CPE_1-T	CPE_1-P	R_{cpp}	R_{pp}	C_{csp}	C_{sp}	W-R	W-T	W-P
(%)	Ω·cm^2	S·cm^{-2}·s^{-n}	-	Ω·cm^2	Ω·cm^2	F·cm^{-2}	F·cm^{-2}	-	-	-
12	82317	2.17×10^{-5}	0.41	3792	1767	2.76×10^{-5}	1.27×10^{-11}			
14	62176	2.12×10^{-5}	0.45	2934	1642	2.48×10^{-5}	1.12×10^{-11}			
16	738	1.93×10^{-5}	0.48	2247	693	2.69×10^{-5}	2.31×10^{-11}	72830	231.4	0.29
18	642	1.73×10^{-5}	0.12	1374	547	3.15×10^{-5}	4.01×10^{-11}	61937	217.8	0.34
20	516	2.19×10^{-5}	0.16	1017	459	4.74×10^{-5}	4.28×10^{-11}	49718	191.5	0.37
Equivalent circuit										

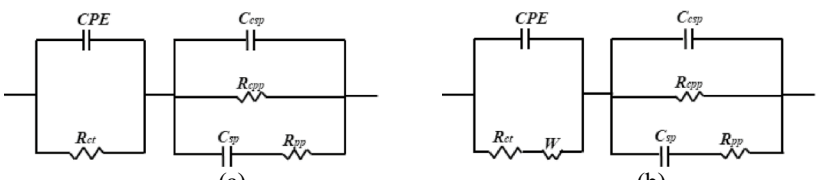

of the soil, combined with the conductive characteristics, the circuit elements inside the soil and the connection between the elements can be predicted, and the ideal equivalent circuit model can be established. Further the circuit elements values are obtained to characterise information such as water content and pore structure to understand the internal structural changes of the soil [34, 37, 44].

Electrochemical impedance spectroscopy (EIS)

Figure 9 shows the EIS of soils with different moisture contents. The Lin-KK degree was used for analyzing the data validity obtained from electrochemical test. The results of the Kramers–Kronig transformation are given in the form of residuals, which the data are valid if they are less than 0.5 [45]. The residuals plot of the electrochemical data of the soil samples are shown in Fig. 10. It can be seen that the residuals of the electrochemical data measured in this study after the Kramers–Kronig transformation are less than 0.5, which indicates that the data are reliable and reasonable.

The Nyquist plot shows capacitive impedance arc in the high-frequency region, the center of the arc is below the abscissa, which corresponds to the non-homogeneous, porous nature of the soil. It is often assumed that the radius of the capacitive arc is related to the charge transfer resistance occurring at the soil-electrode interface, and the value at the intersection of the capacitive arc in high-frequency zone and the abscissa can represent the resistance of the soil [38, 46]. With the increase of the moisture content, the value at the intersection of the Nyquist decreases, which indicates that the impedance of the soil follows a decreasing trend, and at the same time, the radius of the arc in the high-frequency zone is also decreasing, which is in line with the change of the electrical resistivity of the soil.

The Bode plot suggests that the impedance modulus (|Z|) of soil samples in the |Z|—log frequency plot show continuous decreasing trend with increasing frequency and then stabilizes. It can be seen specifically from the Bode plot that the impedance values in the low-frequency region (10^{-1}–10^{3} Hz) decreases more, while the impedance values in the middle-frequency region (10^{3}–10^{4} Hz) and the high-frequency region (10^{4}–10^{5} Hz) remain almost unchanged. With increasing moisture content, the starting point in the low-frequency region of the |Z|-log frequency plot is similar, while the horizontal line in the mid- and high-frequency regions shows a significant downward translation. It shows that the impedance value decreases and the electrical conductivity of the soil increases, which is because pore water is the main factor affecting the electrical conductivity of the soil. Also, the increase of moisture content will make it easier to form connected pore channels in the soil, which in turn affects the electrical conductivity [47].

The presence of 2 time constants is observed in the -theta—log frequency plot and the phase angle reflect the state of the electrode surface [46]. The frequency of the main peaks in the -theta—log frequency plot is mainly concentrated between 10^{0} and 10^{2} Hz, and the frequency of the main peaks shows an increasing trend with the increase of moisture content.

Equivalent circuit model and electrochemical parameters

Factors affecting the electrical conductivity of soil mainly include the conductivity of the pore water and of the double electric layer around the soil particles. Based on the soil conductive paths constructed by some scholars [37, 42, 46] combined with the conductive mode of soil, the equivalent circuit models of the test soil were obtained (Table 3). It is worth noting that the Nyquist plots of soils with moisture content between 16 and 20% in Fig. 9 show an inclined line at low-frequency regions attributed to diffusion impedance in the electrochemical system, and therefore a Warburg impedance (W) was added to the equivalent circuit model. In the equivalent circuit model, R_{csp} is the resistance in the conductive path through the connected soil particles, C_{csp} is the double electric layer capacitance formed on the surface of the clay particles in the connected soil particles, R_{sp} is the discontinuous soil particles resistance in the conductive path of the soil particles and pores in series, C_{sp} is the double electric layer capacitance formed on the surface of clay particles in the discontinuous soil particles, R_{pp} is the discontinuous pore resistance in the conductive path of soil particles and pores in series, R_{cpp} is the connected pore resistance in the conductive path of the connected pores, Rct is the charge transfer resistance and CPE is the constant-phase element.

The Nyquist plots were further fitted by the proposed equivalent circuit models and parameters are given in Table 3. There was an inverse relationship between the pore resistance and the electrical conductivity of the soil. Changes in moisture content significantly affect the change in R_{ct} due to the fact that the reaction zone is filled with more water as the moisture content increases, which increases the number of conductive paths and makes charge transfer easier. The value of C_{csp} is greater than C_{sp}, which indicates that more double electric layers are formed on the surface of clay particles in the conductive path of the connected pores in the soil [48].

The value of R_{cpp} is always greater than R_{pp}, indicating that the electrical conductivity of the soil pore is mainly determined by the connected pores. With the increase of moisture content, the R_{cpp} always shows a decreasing trend, which indicates that the increase of the moisture

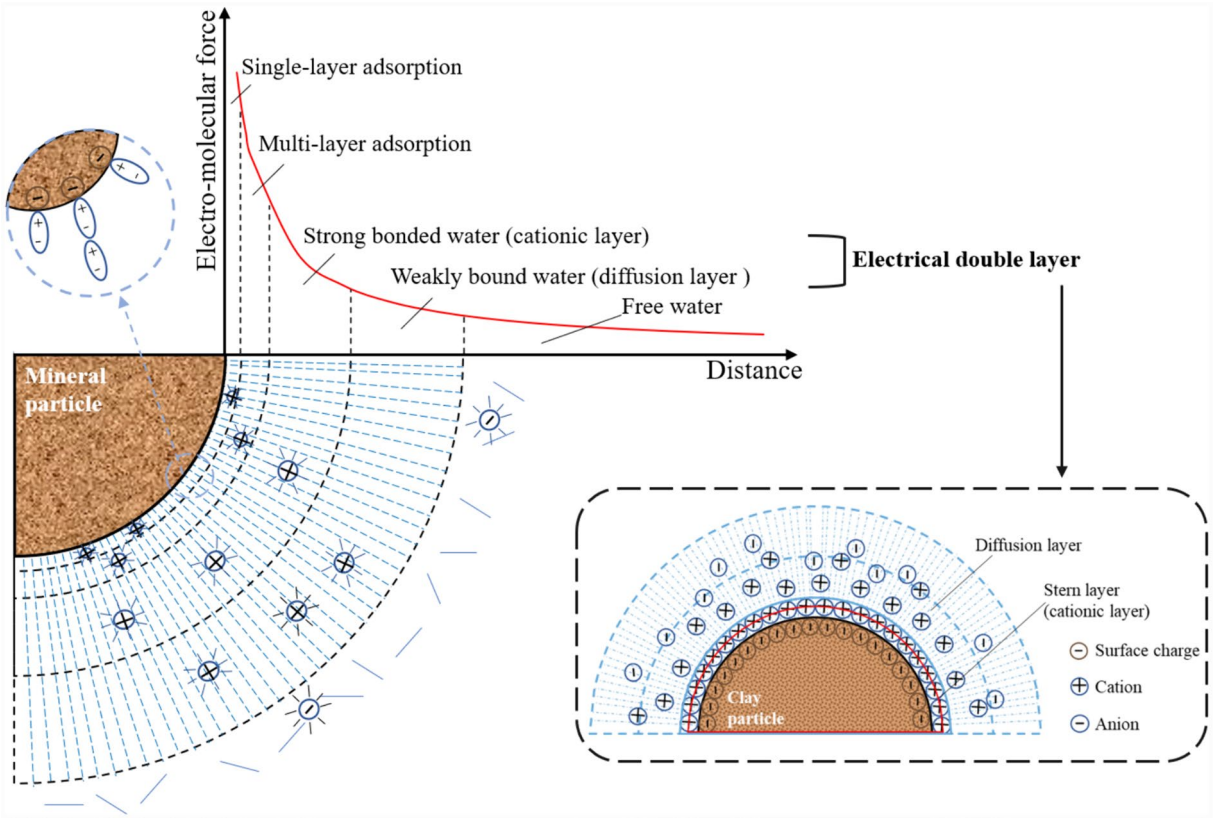

Fig. 11 Modelling of water film on the surface of soil particles

content significantly improves the electrical conductivity of the connected pore channels. The values of R_{cpp} are larger for soils with a low moisture content, and the conductivity of connected pore can change drastically with the addition of small amounts of moisture. This is due to in the soil with low moisture content, moisture is closely adsorbed by the clay minerals to form the inner layer of the double electric layer, the ions are subjected to a strong force, which is suggested the high resistance of the connected pore channels and poor electrical conductivity [49].

With the increase of moisture content, the conductivity of the connected pores is significantly enhanced, and the suction on ions far from the particle surface further decreased [50, 51]. At At this time, the electrical conductivity of the pores was mainly affected by the electrical conductivity of the pore water, and the electrical conductivity of the c continuous pores also tended to be in a steady state [52]. This is also evinced by the variation of C_{csp} with moisture content, where the value of C_{csp} shows an increasing trend, indicating that the double electric layer on the surface of the clay grains in the continuous soil particles is expanding and developing with the increase of the moisture content.

Correlations analysis between the index of water-holding properties and electrochemical parameters

The solid, liquid, and gas phases of the soil each have their own characteristics, and the phases interact with each other, causing changes in the pore characteristics of the soil and making the soil structure more complex. This is the fundamental factor that affects the physical and mechanical properties of the soil and contributes to its water-holding properties and electrochemical characterization.

Figure 11 shows the model of water film on the surface of soil particles. The electrical conductivity of the soil depends mainly on the moisture content, the pore solution and the double electric layer of the soil. Among them, the conductivity of the pore solution comes from the free mobile ions in the solution, and the conductivity of the double electric layer comes from the ion migration.

Since the test soil were prepared using deionized water to obtain the target water content, the effect of ionic conductivity on soil conductivity could be ruled out. It can be inferred that the pore saturation and the state of the adsorbed water layer are the main factors affecting change in the soil conductivity, so the pore resistance was chosen to characterize these factors.

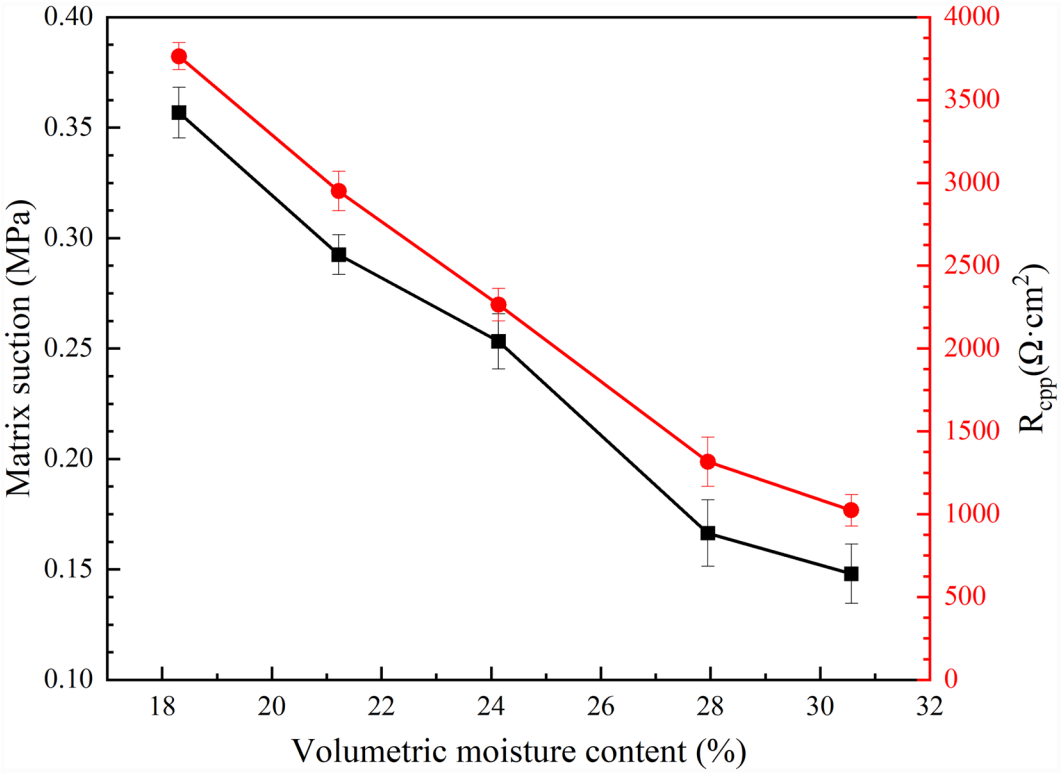

Fig. 12 The correlation of matrix suction and R_{cpp} with the volumetric moisture content

At the same time, the conductive channels within the soil were characterized by electrochemical impedance spectroscopy tests, and the conductive channels were classified into connected pore channel and unconnected pores channel. We find that connected pore resistance (R_{cpp}) is always larger than unconnected pore resistance (R_{pp}) for soils with different moisture contents, indicating that the electrical conductivity of soil is mainly determined by the connected pores.

By comprehensive consideration, the R_{cpp} was selected as the vital parameter that directly influences the electrochemical responses for the correlation analysis between water-holding indicators and electrochemical parameters. Therefore, the volumetric moisture content of the test soil was fitted to the electrochemical parameter R_{cpp}, and the fitting relationship is shown in Fig. 12. The value of R_{cpp} of the soil exhibits a negative power function correlation with the volumetric moisture content.

Soil with low moisture content has large intergranular pores and more interconnected pores, and the surface of the clay particles forms adsorbed water layer and thin strongly bound water layer. These cause the higher capillary increase and higher matric suction in the soil, which in turn cause high pore resistance and poor electrical conductivity of the soil [41]. With increasing moisture content, the thickness of the bound water layer and electrical conductivity of the soil increases, while the adsorption force and matrix suction of soil decreases. At the same time, the connectivity increases and the bonding strength between the soil particles decreases due to thickening of the water film [53].

The existence of an intrinsic relationship between the volumetric moisture content of the soil and the pore resistance and matrix suction further demonstrates that the electrical conductivity occurs mainly through the double electric layer in the connected pore conductive path. The higher the moisture content of the soil led to the lower the connected pore resistance, the higher the electrical conductivity of the connected pore paths, the lower the matrix suction, and the weaker the water-holding capacity of the soil. The connected pore resistance can characterize the changes in the electrical conductivity of the soil as well as the changes in the water-holding capacity of the soil, so the electrochemical detection can

be applied to monitor the changes in the water-holding properties of the soil under the cultural relics.

Conclusion

The study summarizes the main deterioration problems of the cultural relics in the Grand Deliverance Hall and the cultural relics in the hall, and concludes that the main factor affecting the generation and development of deterioration is groundwater erosion through environmental monitoring and geotechnical engineering investigation. The impact of changes in moisture content on the water-holding properties and pore distribution of the soil under the cultural-relics buildings was further assessed. Then, combined with the soil property, this study provides a novel way to reflect the water-holding properties of the soil using electrochemical detection. The specific conclusions reached are as follows.

(1) The moisture content has a significant effect on the water-holding properties of the soil. The matrix suction of the soil tended to decrease with increasing moisture content and the rate of decrease gradually slowed down.
(2) Pore structure and moisture content are the main factors affecting the electrochemical characteristics of the soil. With the increase of moisture content, the connected pore resistance decreases and the electrical conductivity of the connected pore paths increases.
(3) The connected pore resistance and matrix suction decrease with the increase in the moisture content, both showing a power function law. Changes in moisture content cause changes in the thickness of the double electric layer, which in turn affects the connected pore resistance and matrix suction of soil. The greater the connected pore resistance, the greater the matrix suction and the water-holding capacity. The electrochemical parameter can be used to characterize the water-holding capacity of the soil, which means that the electrochemical detection can be applied to monitor and reflect the water-holding properties of the soil under the cultural-relics buildings.

Recommendations and inspirations for the prevention of groundwater erosion in historic buildings

Cultural-relic buildings are susceptible to deterioration under the influence of groundwater erosion, and it is crucial to propose protective measures for preventing deterioration. Based on the research of this study and the conservation ideology of cultural relics that respects the original and minimizes intervention, the proposed measures to prevent groundwater erosion include the following aspects.

(1) Electrochemical detection is a novel and effective way to monitor and reflect the water-holding properties of the soil under the cultural-relic buildings. Periodically recording and evaluating the electrochemical characteristics of the soil under the buildings, and further characterizing and reflecting the water-holding properties of the soil. In this way, it is possible to detect changes in the water-holding properties of the soil in time for protective measures to be carried out in a scientific and targeted manner. For example, when the hidden danger of groundwater erosion is found, adequate ventilation and air circulation measures can be provided to ensure that the cultural-relic are dry, to inhibit deterioration due to excessive humidity inside the heritage buildings, and to prevent the occurrence of further structural problems.
(2) For the groundwater erosion caused by cultural-relic have appeared structural damage and strength deterioration, it is recommended that the use of suitable materials combined with the traditional technology for emergency repair. Our research group is collecting further data for construct evaluation model to comprehensive prediction and evaluation of the deterioration degree under groundwater erosion, and carry out targeted research on modified materials to improve the water resistance and durability of the cultural-relic buildings. This study can provide preliminary data and a research basis for the test considering the structural characteristics of cultural relics under the influence of groundwater erosion.

Abbreviations

WHC	World heritage committee
ICCROM	International center for the study of the preservation and restoration of cultural property
ICOMOS	International council on monuments and sites
EIS	Electrochemical impedance spectroscopy
SWCC	Soil–water characteristic curves
SCE	Saturated calomel electrode
WE	Working electrode
CE	Counter electrode
RE	Reference electrode

Acknowledgements

We thank the Comprehensive Research Project on the Grand Deliverance Hall at the Chongshan Temple (2023KT02, Shanxi Provincial Bureau of Cultural Relics scientific research topics) and the Damage Mechanism and Protection of Harmful Dirt on the Surface of Color Plastic Sculptures in Chongshan Temple, Taiyuan, China (20210302124453, Fundamental Research Program of Shanxi Province) for the assistance in this study.

Author contributions
L.Y., B.X., W.X., H.L., B.X.J., H.P. and A.Y. conceptualized the study. L.Y. and B.X., was primarily responsible for conducting the investigation and analysis, which included experimental design, data analysis, diagram creation, and manuscript writing. W.X. and H.P. was assigned with the task of reviewing and revising the manuscript. H. L. and B.X.J. was in charge of maintaining and sampling the experimental plot, while W.X. and A.Y. assumed responsibility for selecting and maintaining the experimental plots. All authors reviewed the manuscript.

Availability of data and materials
All data generated or analyzed during this study are included in this published article.

Declarations

Competing interests
The authors declare no competing interests.

Author details
[1]Shanxi Academy of Ancient Building, Painted Sculpture and Mural Preservation, Taiyuan 030012, Shanxi, People's Republic of China. [2]College of Civil Engineering, Taiyuan University of Technology, Taiyuan 030024, Shanxi, People's Republic of China. [3]National Demonstration Center for Experimental Design and Art Education, Taiyuan University of Technology, Taiyuan 030024, Shanxi, People's Republic of China.

Received: 27 January 2024 Accepted: 20 June 2024
Published online: 04 July 2024

References

1. Wang BS, Dai L, Liao BJ. System architecture design of a multimedia platform to increase awareness of cultural heritage: a case study of sustainable cultural heritage. Sustainability. 2023;15(3):2504.
2. Trček D. Cultural heritage preservation by using blockchain technologies. Herit Sci. 2022;10:6.
3. Skublewska-Paszkowska M, Milosz M, Powroznik P, Lukasik E. 3D technologies for intangible cultural heritage preservation—literature review for selected databases. Herit Sci. 2022;10:3.
4. Cigna F, Tapete D, Lee K. Geological hazards in the UNESCO world heritage sites of the UK: from the global to the local scale perspective. Earth-Sci Rev. 2018;176:166–94.
5. Baglioni M, Poggi G, Chelazzi D, Baglioni P. Advanced materials in cultural heritage conservation. Molecules. 2021;26(13):3967.
6. Jalón ML, Chiachío J, Gil-Martín LM, Hernández-Montes E. Probabilistic identification of surface recession patterns in heritage buildings based on digital photogrammetry. J Build Eng. 2021;34:101922.
7. Frodella W, Elashvili M, Spizzichino D, Gigli G, Nadaraia A, Kirkitadze G, Adikashvili L, Margottini C, Antidze N, Casagli N. Applying close range non-destructive techniques for the detection of conservation problems in rock-carved cultural heritage sites. Remote Sens. 2021;13(5):1040.
8. Luo Y, Zhou PS, Ni PP, Peng XQ, Ye JJ. Degradation of rammed earth under soluble salts attack and drying-wetting cycles: the case of Fujian Tulou, China. Appl Clay Sci. 2021;212:106202.
9. Umubyeyi C, Wenger K, Dahmen J, Ochsendorf J. Durability of unstabilized rammed earth in temperate climates: a long term study. Constr Build Mater. 2023;209:133953.
10. Bay E, Martinez-Molina A, Dupont WA. Assessment of natural ventilation strategies in historic buildings in a hot and humid climate using energy and CFD simulations. J Build Eng. 2022;51:104287.
11. Mi XC, Li YQ, Qin XC, Li J. Effects of natural weathering on aged wood from historic wooden building: diagnosis of the oxidative degradation. Herit Sci. 2023;11:109.
12. Varas-Muriel MJ, Fort R, Martínez-Garrido MI, Zornoza-Indart A, López-Arce P. Fluctuations in the indoor environment in Spanish rural churches and their effects on heritage conservation: hygro-thermal and CO_2 conditions monitoring. Build Environ. 2014;82:97–109.
13. Coelho GBA, Silva HE, Henriques FMA. Impact of climate change in cultural heritage: from energy consumption to artefacts' conservation and building rehabilitation. Energ Build. 2020;22:110250.
14. Cui K, Wu GP, Du YM, An XY, Wang ZL. The coupling effects of freeze-thaw cycles and salinization due to snowfall on the rammed earth used in historical freeze-thaw cycles relics in northwest China. Cold Reg Sci Technol. 2019;160:288–99.
15. Melin CB, Bjurman J. Moisture gradients in wood subjected to relative humidity and temperatures simulating indoor climate variations as found in museums and historic buildings. J Cult Herit. 2017;25:157–62.
16. Varas-Muriel MJ, Fort R, Gómez-Heras M. Assessment of an underfloor heating system in a restored chapel: balancing thermal comfort and historic heritage conservation. Energ Build. 2021;251:111361.
17. Scott DA. Conservation and authenticity: interactions and enquiries. Stud Conserv. 2015;60(5):291–305.
18. Philokyprou M, Limbouri-Kozakou E. An overview of the restoration of monuments and listed buildings in Cyprus from antiquity until the twenty-first century. Stud Conserv. 2015;60(5):267–77.
19. Chen S, Chen J, Jiming Y, Wang T, Jian X. Prediction of deterioration level of heritage buildings using a logistic regression model. Buildings. 2023;13(4):1006.
20. Drobiec L, Grzyb K, Zając J. Analysis of reasons for the structural collapse of historic buildings. Sustainability. 2021;13(18):10058.
21. Hatır ME, Korkanç M, Başar ME. Evaluating the deterioration effects of building stones using NDT: the Küçükköy Church, Cappadocia Region, central Turkey. B Eng Geol Environ. 2019;78:3465–78.
22. Riminesi C, Cuzman OA, Moczko M, Raszczuk K. Comparative interpretation of results after application of different non-destructive and portable techniques on historic concrete in the centennial hall in Wrocław. Case Stud Constr Mat. 2022;17:e01409.
23. Orr SA, Fusade L, Young M, Stelfox D, Leslie A, Curran J, Viles H. Moisture monitoring of stone masonry: a comparison of microwave and radar on a granite wall and a sandstone tower. J Cult Herit. 2020;41:61–73.
24. Feng ZB, Luo LX, Wang JQ, Cao SJ. Energy-efficient preservation environment control for enclosed exhibition hall of earthen relics. Energ Build. 2022;256:111713.
25. Brimblecombe P, Hayashi M, Futagami Y. Mapping climate change, natural hazards and Tokyo's built heritage. Atmosphere. 2020;11(7):680.
26. Raszczuk K, Karolak A. Correlation between the cracking pattern of historical structure and soil properties: the case of the church in Kożuchów. Herit Sci. 2021;9:43.
27. Siedel H. Historic building stones and flooding: changes of physical properties due to water saturation. J Perform Constr Fac. 2010;24(5):452–61.
28. Chang LH, Chang XH, Chang H, Qian W, Cheng LT, Han XL. Nondestructive testing on ancient wooden components based on Shapley value. Adv Mater Sci Eng. 2019. https://doi.org/10.1155/2019/8039734.
29. Ma XY, Xia DS, Zhang GB, Chen PY, Liu XY, Liu H, Wang WF, Zhan HT, Zhang YX, Yu Q. Water-soluble ions and heavy metal levels, source apportionment, and health risk of indoor dust in the Mogao Grottoes of Dunhuang, China. Indoor Air. 2023. https://doi.org/10.1155/2023/4818195.
30. Wood JD, Gauvin C, Young CRT, Taylor AC, Balint DS, Charalambides MN. Reconstruction of historical temperature and relative humidity cycles within Knole House. Kent J Cult Herit. 2019;39:212–20.
31. Boesgaard C, Hansen BV, Kejser UB, Mollerup SH, Ryhl-Svendsen M, Torp-Smith N. Prediction of the indoor climate in cultural heritage buildings through machine learning: first results from two field tests. Herit Sci. 2022;10:176.
32. Proietti N, Calicchia P, Colao F, Simone SD, Tullio VD, Luvidi L, Prestileo F, Romani M, Tatì A. Moisture damage in ancient masonry: a multidisciplinary approach for in situ diagnostics. Minerals. 2021;11(4):406.
33. Mu QY, Ng CWW, Zhou C, Zhou GGD. Effects of clay content on the volumetric behavior of loess under heating-cooling cycles. J Zhejiang Univ-SC A. 2019;20:979–90.
34. Dong H, Zhu XM, Jiang XZ, Chen L, Gao QF. Structural characteristics of soil-rock mixtures based on electrochemical impedance spectroscopy. CATENA. 2021;207:105579.
35. Barsoukov E, Macdonald JR. Impedance spectroscopy theory, experiment, and applications[M]. Hoboken: John Wiley & Sons, Inc.; 2018.

36. Cabeza M, Keddam M, NovoaX R, et al. Impedance spectroscopy to charactrize the pore structure during the hardening process of portland cement paste[J]. Electrochim Acta. 2006;51(8–9):1831–41.
37. Han PJ, Zhang YF, Chen FY, Bai XH. Interpretation of electrochemical impedance spectroscopy (EIS) circuit model for soils. J Cent South Univ. 2015;22:4318–28.
38. Wang K, Hui Y, Zhou C, Li X, Rong Y. Soil-water characteristic surface model of soil-rock mixture. J Mt Sc. 2023;20:2756–68.
39. Al-Mahbashi AM, Elkady TY, Alrefeai TO. Soil water characteristic curve and improvement in lime treated expansive soil. Geomech Eng. 2015;8(5):687–706.
40. Lu N. Generalized soil water retention equation for adsorption and capillarity. J Geotech Geoenviron. 2016;142(10):04016051.
41. Wen TD, Wang PP, Shao LT, Guo XX. Experimental investigations of soil shrinkage characteristics and their effects on the soil water characteristic curve. Eng Geol. 2021;284:106035.
42. Chen ZW, Han PJ, He B, Sun FN, Bai XL, Liu XY, Wang YT. Electrochemical impedance spectroscopy study of lime soil and interpretation of the results. Int J Electrochem Sc. 2021;16(8):210819.
43. Li XJ, Wang X, Zhao Q, Zhang YY, Zhou QX. In situ representation of soil/sediment conductivity using electrochemical impedance spectroscopy. Sensors. 2016;16(5):625.
44. Chen ZW, Han PJ, He B, Sun FN, Bai XL, Wang XY, Guo TT, Wang XY. Electrochemical impedance spectroscopy (EIS) of NaCl-saturated sandy soil at sub-zero temperatures. Int J Electrochem Sc. 2021;16(9):210914.
45. Lasia A. Electrochemical impedance spectroscopy and its applications[M]. New York: Springer; 2014.
46. Han PJ, Chen FY, Ren C, Bai XH. Electrochemical impedance spectroscopy of hardened compacted cemented soils at early curing stage. Mater Test. 2015;57(4):343–8.
47. Xie RZ, Xie YT, Li BQ, Han PJ, He B, Dou BJ, Bai XH. Electrochemical impedance spectroscopy of sandy soil containing Cl^-, SO_4^{2-} and HCO_3^-. Int J Electrochem Sc. 2021;16(12):211211.
48. Peng SQ, Wang F, Fan L. Study on electrochemical impedance response of sulfate saline soil. Int J Electrochem Sc. 2019;14(9):8611–23.
49. Gong WP, Quan C, Li XX, Wang L, Zhao C. Statistical analysis on the relationship between shear strength and water saturation of cohesive soils. B Eng Geol Environ. 2022;81:337.
50. Lu Y, Liu SH, Zhang YG, Wang LJ, Li Z. Hydraulic conductivity of gravelly soils with various coarse particle contents subjected to freeze–thaw cycles. J Hydrol. 2021;598:126302.
51. Chen ZX, Yu HY, Wan Y, He XX, Hua LF. Temperature-dependent relationship between soil water content and electrical conductivity. Environ Geotech. 2023. https://doi.org/10.1680/jenge.23.00013.
52. Tan X, Wu JW, Huang JS, Wu MS, Zeng WZ. Design of a new TDR probe to measure water content and electrical conductivity in highly saline soils. J Soil Sediment. 2018;18:1087–99.
53. Yu HY, Chen ZX, Wan Y, Sun X. Temperature-humidity-density dependent evaporation behaviour of clay and sandy clay[J]. Eur J Soil Sci. 2024;75(2):e13484.

Publisher's Note